

# Analysis of Influence of Strain Gage Rosette on Relieved Strain

Patrik Šarga\*, Peter Senko, František Trebuňa

Department of Applied Mechanics and Mechatronics, Technical university in Košice, Faculty of Mechanical Engineering,; Letná 9, 040 01 Košice, Slovakia

\*Corresponding author: patrik.sarga@tuke.sk

Received October 14, 2013; Revised October 17, 2013; Accepted November 11, 2013

**Abstract** Hole-drilling method is the most widely used method for measuring residual stresses. This method is performed using strain gage rosette attached to the surface of the studied components, through which we drill blind or through-hole. This paper is devoted to analyzing of influence of strain gage rosette on relieved strain. Our aim was to establish more accurately model of strain gage rosette, and examine its effect on hardening of the surface around the hole. For modeling by FEM was used strain gage rosette RY 21 made by HBM.

**Keywords:** residual stress, hole-drilling method, strain gage rosette, FEM (finite element method)

**Cite This Article:** Patrik Šarga, Peter Senko<sup>1</sup> and František Trebuňa, “Analysis of Influence of Strain Gage Rosette on Relieved Strain.” *American Journal of Mechanical Engineering* 1, no. 7 (2013): 309-312. doi: 10.12691/ajme-1-7-31.

## 1. Introduction

The residual stresses [4] are the stresses that exist in object in the absence of external loading. These stresses are generated by technological process or by previous loading. In principle all technological processes - rolling, forming and thermal processing etc. - generate in produced object residual stresses. There are a number of destructive and non-destructive methods, which are used for determination of residual stresses. One of them is hole-drilling method. This method is semi destructive and its principle is based on drilling of a small hole to the center of strain gage rosette. When the material removed by drilling, relieved strains are recorded by the strain gage rosette, from which we can calculate the direction and size of the principal stresses. Hole-drilling method is usable for homogenous and non-homogenous residual stresses [1,2,3].

### 1.1. Input Parameters

As a model for our analysis we created in software COSMOS / M, rectangular plate with dimensions 53x53x0.3 mm, and we loaded this plate in the x direction by stress  $\sigma = 100$  MPa. After that we drilled hole in the middle of strain gage rosette. We used a strain gage rosette RY21 made by HBM Figure 1.

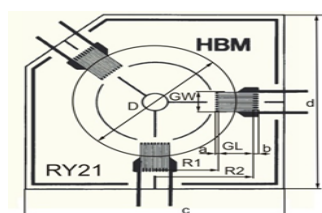


Figure 1. Strain gage rosette RY21

Strain gage rosette dimensions:

$D = 13$  mm,  $R1 = 5$  mm,  $b = 0.5$  mm,

$GL = 3$  mm,  $R2 = 8$  mm,  $c = 22$  mm,

$GW = 2.5$  mm,  $a = 0.25$  mm,  $d = 22$  mm,

$Do = 0.5 \cdot D = 6.5$  mm.

Thickness of constantan strain gage foil is 0.01 mm; thickness of adhesive is 0.2mm.

The materials that make up the strain gage rosette and their properties are listed in Table 1.

Table 1. Used materials

Material	E [MPa]	$\mu$
Steel	$2.1 \cdot 10^5$	0.3
Constantan	$1.62 \cdot 10^5$	0.33
Polyamide	$5.5 \cdot 10^3$	0.38

## 2. Theoretical Calculation of Strains in the X-Direction

Figure 2 shows a strain gage, which is divided by the grid to the individual wires. Each wire is divided into 17 sections. The points of intersections of the longitudinal and transverse lines are forming nodes, in which we determine a strain.

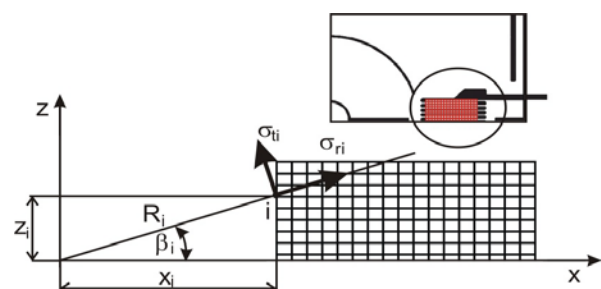


Figure 2. Model of the strain gage

Thus we obtained in each grid point the value of the elongation  $\epsilon_x$  in the direction of the x axis. The software COSMOS / M allows us to obtain only the average value of strain in the element, and therefore it is necessary to make the average values of strains in the neighboring points so that we can compare the results [6].

Obtained values are shown in Figure 3 and Figure 4 [5]. Longitudinal wires of strain gage are numbered counterclockwise, and because of strain gage symmetry, numbering starts from the midline of the strain gage from 1 to 9. Each wire consists of 17 elements, which are numbered 1–7 from the center of the hole.

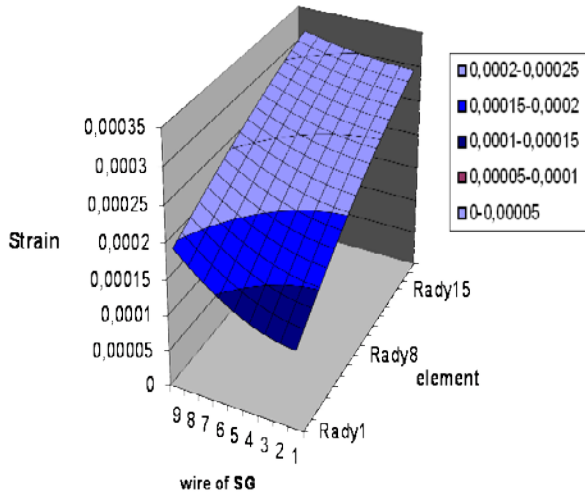


Figure 3. Field of strain in the strain gage

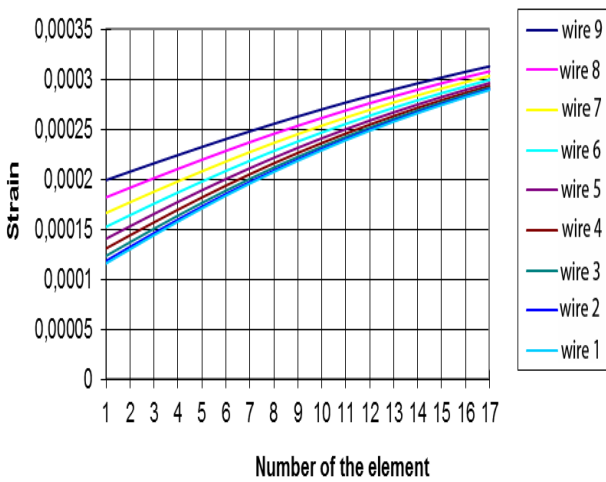


Figure 4. Strain of the strain gage wires designed by theoretical calculation

Now we compare the results of theoretical computation with the model of strain gage created by using FEM.

**2.1. Solution by FEM**

For modeling of strain gage grid we used element (in the program COSMOS / M marked as TRUSS2D). This feature allows us a simple data entry of material properties of the grid and also simple reading of strain. To become as close as possible to theoretical solution, it is necessary that strain gage does not solidify the area around the hole. Therefore the grid elastic modulus is set to  $E = 1.10 \cdot 6$  MPa.

Finite element mesh is shown in Figure 5

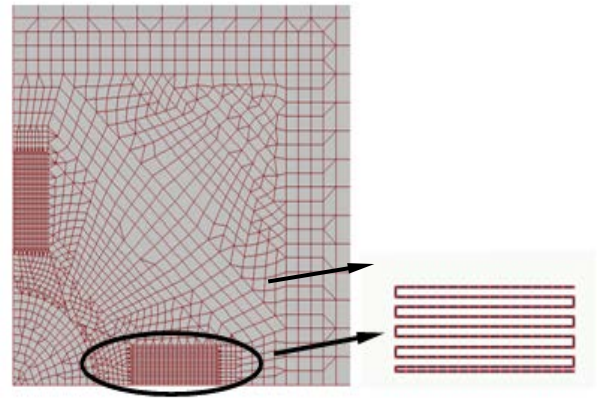


Figure 5. Finite element mesh used for the model of strain gage rosette

Field of strains in the direction of the x-axis is in Figure 6.

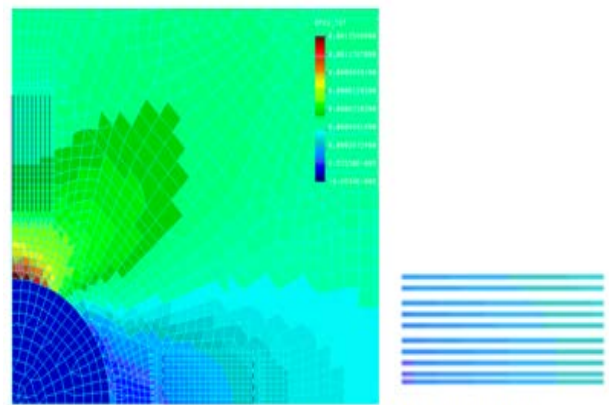


Figure 6. Field of strains around the hole drilling

Strains of the finite elements model of strain gage is shown in Figure 7.

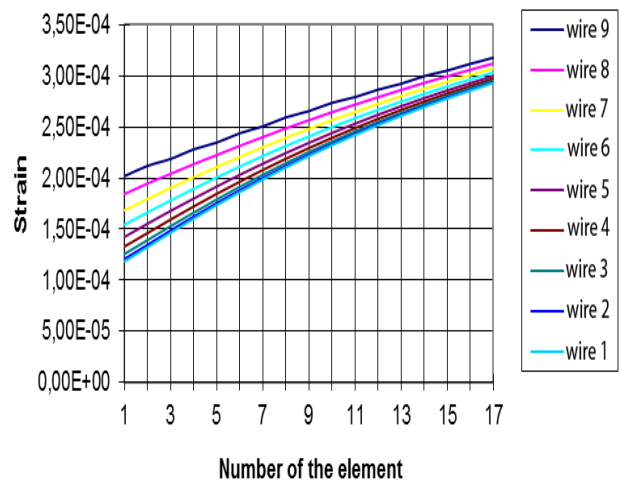


Figure 7. Strains in each strain gage wires designed using FEM

For comparison of the theoretical solution with the solution using FEM see Figure 8 illustrating strains in the direction of the x-axis wires 1, 5 and 9.

Deviation of strains identified by FEM from the theoretical solution is an average of 1.2%. Effect of strain gage rosette on the strain in the drill hole we investigated by using FEM model. The grid of strain gage we modeled using beam members, similarly as in the previous case. Dimensions of wire depend on the dimensions of strain gage rosette.

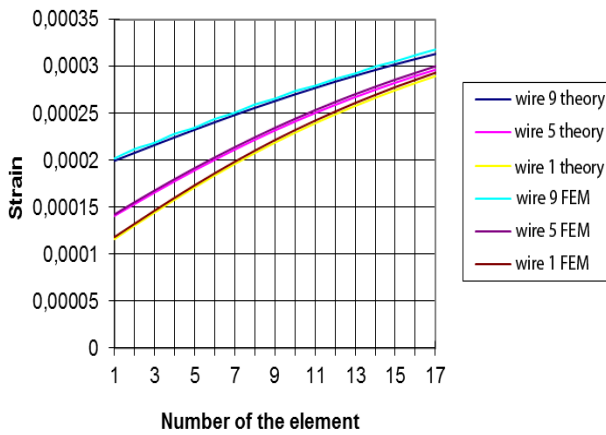


Figure 8. Comparison of strains in 3 wires

The longitudinal wires have the cross-section  $0.0005 \text{ mm}^2$ , transverse inner edge wires have  $0.0025 \text{ mm}^2$  and the outer edge wires have  $0.005 \text{ mm}^2$  cross-section. Material of the wire is constantan with material properties according to Table 1. The base of strain gage we modeled together with glue. For a model base we used the shell element (SHELL4). Thickness of the strain gage base with adhesive is 0.2 mm. Material of the base is polyamide with properties according to Table 1. Plate dimensions and also the dimensions of strain gage rosette are the same as in the previous case.

Finite element mesh is shown in Figure 9.

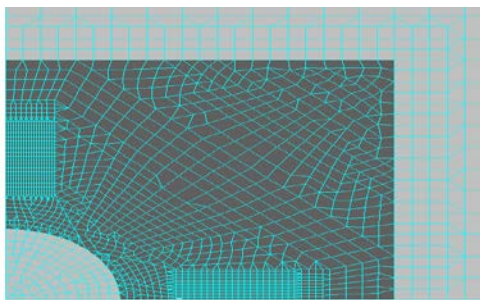


Figure 9. Model of the strain gage rosette with reinforcement

The dark part on the Figure 9 shows the base of the strain gage rosette together with glue. We observed the effect of reinforcement by the strain gage rosette around the hole. After that we compared the results of reinforcement by strain gage rosette using FEM with the FEM solution without reinforcement. The deviation is shown in Figure 10.

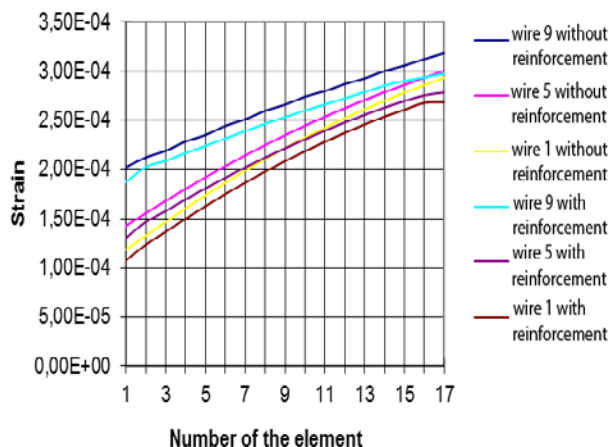


Figure 10. Comparison of strains in the three wires with and without reinforcement by strain gage rosette

As shown in Figure 10, usage of a specific strain gage rosette leads to solidification of the material around the hole. The average deviation between calculations with and without reinforcement is 5.9 %.

In the next part we observed what effect has reinforcement of the material by the strain gage rosette around the hole in each step of drilling.

As a model we used a rectangular plate with dimensions  $53 \times 53 \times 0.8 \text{ mm}$ . Finite element mesh has 8 layers and each layer represents each step of drilling. It means that each step of drilling is 0.1 mm. We created two models. The first one is the plate without reinforcement by the strain gage rosette, which was built in the same manner as in the previous case. The second model is a plate with reinforcement by the strain gage rosette. Material of the rosette and plate is in Table 1. Model of the plate is shown in Figure 11.

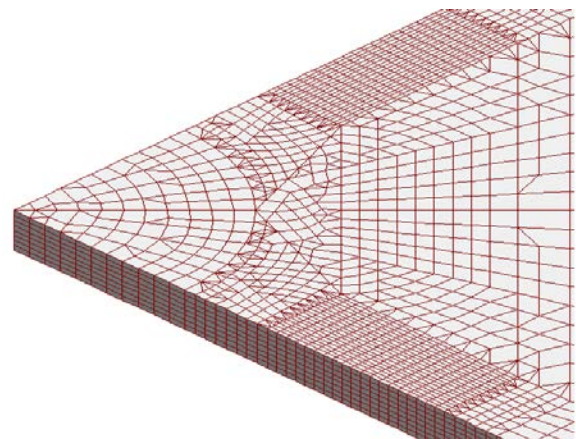


Figure 11. Finite element mesh of the strain gage rosette

Because there is no theoretical solution, we relied on the fact that the deviation from the theoretical solution and FEM solution without reinforcement is less than 1.2% as it was in the previous case.

We observed the value of strains  $\epsilon_x$  in all finite elements of the strain gage rosette. From these values we calculated the average value of the strains in the particular depths of the hole. The same procedure was made also with model with reinforcement. After that we compared the results with and without reinforcement. The results are in Table 2.

Table 2. The values  $\epsilon_x$  in the different depths of the specimen with and without reinforcement by the strain gage rosette

Depth [mm]	0.1	0.2	0.3	0.4	0.5	0.6	0.7	0.8
$\epsilon_x (10^4)$ without reinforcement	4.46	4.06	3.62	3.20	2.85	2.58	2.38	2.31
$\epsilon_x (10^4)$ with reinforcement	4.34	3.95	3.53	3.12	2.78	2.52	2.32	2.25
Deviation (%)	2.60	2.58	2.51	2.41	2.33	2.33	2.40	2.59

Deviation is shown in Figure 12.

Figure 12 shows that the value of the deviation with depth of drilling remains practically unchanged and its value is about 2.5%. This implies that the reinforcement of

the sample by this specific strain gage rosette depends on thickness of the sample, in which the hole is drilled.

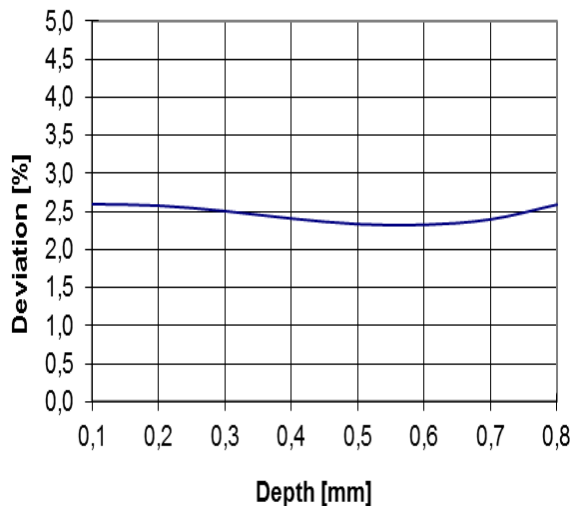


Figure 12. Changing of the deviation over the thickness of the plate

With magnification of sample thickness from 0.3 mm to 0.8 mm the deviation changed from 5.9% to 2.5%. We can deduce that with the reduction of the thickness of the sample the reinforcement is growing.

To determine the relationship between the thickness of the sample and deviation, we used the model in Figure 9. This model was used for modeling the plates of different thicknesses.

The results of the drilling were compared with the solution using FEM without reinforcement. The results obtained are shown in Table 3.

Table 3. The values  $\varepsilon_x$  for the various thickness of the specimen with and without reinforcement by the strain gage rosette

Thickness [mm]	0.1	0.2	0.3	0.4	0.5
$\varepsilon_x (10^4)$ without reinforcement	2.00	2.12	2.18	2.21	2.23
$\varepsilon_x (10^4)$ with reinforcement	2.32	2.32	2.32	2.32	2.32
Deviation (%)	13.92	8.39	5.97	4.65	3.85
Thickness [mm]	0.6	0.7	0.8	0.9	1.0
$\varepsilon_x (10^4)$ without reinforcement	2.24	2.25	2.25	2.26	2.26
$\varepsilon_x (10^4)$ with reinforcement	2.32	2.32	2.32	2.32	2.32
Deviation (%)	3.31	2.94	2.59	2.48	2.35

Relationship between thickness of the specimen and the deviation is shown in Figure 13.

As shown in Figure 13 with increasing thickness of the specimen the deviation decreases.

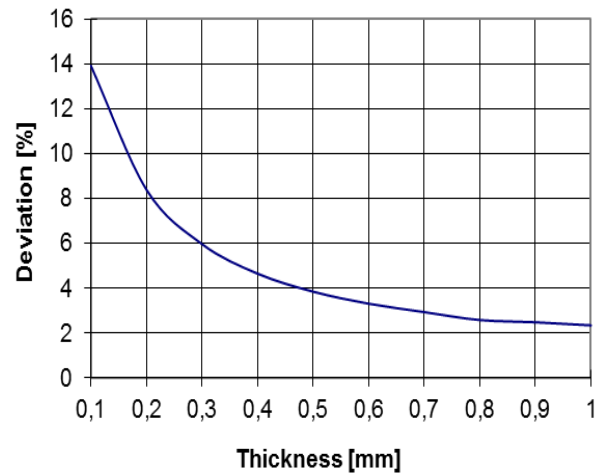


Figure 13. Effect of thickness of specimen on hardening by strain gage rosette

### 3. Conclusion

Residual stresses deserve big attention. Usually they are undesirable, it is difficult to identify them and expensive to remove them. Their presence can be harmful in large components and supporting structures such as vehicles or components of nuclear reactors, stands production machinery, bridges etc. The severity of their occurrence associated with limited options for its measuring and removing points out that we must pay attention to them. In most cases, it is difficult to determine residual stresses analytically. For this reason, experimental methods for the determination of residual stress are still very important.

The results of this paper are incorporated into the software MEZVYNA [7] for determination of residual stresses, which is developed at our department.

### Acknowledgement

This work was supported by the Ministry of Education of the Slovakia Foundation under Grant VEGA No. 1/0289/11, VEGA No. 1/0937/12 and APVV-0091-11 and by project " Research modules for intelligent robotic systems " (IMTS: 26220220141), on the basis of Operational Program Research and Development financed by European Regional Development Fund.

### References

- [1] ASTM Standard E837-08.
- [2] Flaman, M.T., Manning, B.H.: Determination of Residual Stress Variation with Depth by the Hole-Drilling Method, Experimental Mechanics, No. 25, 1985.
- [3] Manning, B. W., Flaman, M. T.: Finite-Element Calculations of Calibration Constants for Determination of Residual Stresses with Depth by the Hole-Drilling Method. Ontario Hydro (Research Division) Report 82-88-K, Toronto, Canada, 1982.
- [4] Lu, J.: Handbook of measurement of residual stresses. Society for experimental mechanics, Fairmont press Liburn, GA, 1996, Chapter 2.
- [5] Senko, P.: Verifikácia určovania zvyškových napätí v závislosti na hĺbke odvrťovania. DDP TU v Košiciach, September 2005.
- [6] Schajer, G. S.: Application of finite element calculations to residual stress measurements. Journal of engineering materials and technology, Transaction, ASME, 103, April 1981, 157-163.
- [7] Šarga, P.: Riadenie odvrťovania a vyhodnocovania zvyškových napätí, DDP TU v Košiciach, September 2005.